Quantitative Evaluation of Microcrack by Acoustic Emission Analysis

T. KISHI and M. ENOKI
Research Center for Advanced Science and Technology, University of Tokyo, Meguro-ku, Tokyo 153, Japan

ABSTRACT

The method to represent a general infinitesimal deformation as a deformation moment tensor has been proposed. Developing the measuring and analysis system for acoustic emission waveform analysis, these moment tensor components due to microcracking can be determined experimentally. The remarkable method in this study is established to evaluate the moment tensor with the dynamic Green's function of finite media by computer simulation using a finite difference method and the deconvolution with multiple Green's function. In addition to three dimensional location of these microcracks, fracture mode, orientation, size and nucleation time of microcracks can be estimated from the obtained moment tensor.

KEYWORDS

Acoustic emission; source characterization; microcracking.

INTRODUCTION

In any case for the purpose to understand both fracture mechanism and toughening mechanism, it is necessary to establish the method to quantitatively evaluate microcracks. In the fields of micromechanics and seismology the deformation such as the above mentioned microcracks have been formulated analytically. Those deformations in materials can be generally represented as nonelastic 'eigenstrain' in micromechanics (Mura, 1982). Acoustic emission (AE) technique has been used as an almost unique method to detect dynamic deformation and fracture of materials with high sensitivity. A few studies (Wadley et al., 1981, Kishi et al., 1983, Scruby et al., 1986) have attempted to characterize acoustic emission sources quantitatively on the analogy of seismology (Aki et al., 1980).

We have represented an infinitesimal deformation in materials as a dynamic eigenstrain and proposed the deformation moment tensor as the physical quantity to uniquely describe such a deformation (Enoki et al., 1988). In this paper, we discuss the developed experimental system and analysis method to determine the moment tensor due to microcracking experimentally in accordance with the AE method, and the microcrack characteristics, such as location, fracture mode, orientation, size and nucleation time.

THEORY OF ACOUSTIC EMISSION

Eigenstrain and Deformation Moment Tensor

Let V denote an elastic domain occupied by a given three dimensional body and $\epsilon^*_{mn}(\mathbf{x}, t)$ denote an eigenstrain tensor in V. Then we can state the displacement field due to $\epsilon^*_{mn}(\mathbf{x}, t)$ as (Mura, 1982)

$$u_i(\mathbf{x}', t) = \int_V C_{jkmn}\ \epsilon^*_{mn}(\mathbf{x}, t) * G_{ij,k}(\mathbf{x}', \mathbf{x}, t)\ dV(\mathbf{x}), \qquad (1)$$

where C_{jkmn} is the elastic stiffness tensor, $G_{ij}(\mathbf{x}', \mathbf{x}, t)$ is the displacement field in the direction x_i at position $\mathbf{x}'$ at the time t due to an impulsive force in the direction x_j at $\mathbf{x}$ at time 0, the comma indicates a differentiation and * means a convolution integral with respect to time. If the dimension of region occupied by eigenstrain $\epsilon^*_{mn}(\mathbf{x}, t)$ is small compared with distance between the position $\mathbf{x}$ and $\mathbf{x}'$, and the shortest wavelength due to $\epsilon^*_{mn}(\mathbf{x}, t)$, then the point source approximation is applied. We can finally state the displacement field due to eigenstrain as

$$u_i(\mathbf{x}', t) = G_{ij,k}(\mathbf{x}', \mathbf{x}, t) * D_{jk}(\mathbf{x}, t), \qquad (2)$$

where deformation moment tensor $D_{jk}(\mathbf{x}, t)$, which is the quantity to represent an infinitesimal deformation, is defined as

$$D_{jk}(\mathbf{x}, t) = \int_V C_{jkmn}\ \epsilon^*_{mn}(\mathbf{x}'', t)\ dV(\mathbf{x}'') = C_{jkmn}\ \epsilon^*_{mn}(\mathbf{x}, t)\ dV, \qquad (3)$$

where dV is the volume of deformation domain. Denoting the Lamé's constants for isotropic materials by λ and μ, we can find

$$D_{jk}(\mathbf{x}, t) = (\lambda\ \epsilon^*_{mm}\delta_{jk} + 2\mu\ \epsilon^*_{jk})\ dV. \qquad (4)$$

Microcracking

It is well known that the generation of microcrack can be modeled as the discontinuity of displacement on the faulting surface like a dislocation. Eigenstrain $\epsilon^*_{ij}(\mathbf{x}, t)$ due to the discontinuity of displacement can be represented as

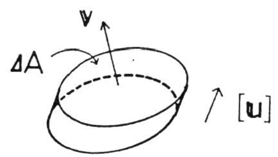

Fig. 1. A microcracking which is modeled as a dislocation source with a fault surface ΔA, normal vector ν_i and displacement discontinuity $[u_i]$.

$$\epsilon^*_{ij}(\mathbf{x}, t) = (1/2)\{[u_i(\mathbf{x}, t)]\ \nu_j(\mathbf{x}) + [u_j(\mathbf{x}, t)]\ \nu_i(\mathbf{x})\}\ \delta(\mathbf{A} - \mathbf{x}), \qquad (5)$$

where $[u_i(\mathbf{x}, t)]$ is the discontinuity of displacement on a surface A, $\nu_i(\mathbf{x})$ is the normal to surface A, which is shown in Fig. 1. And $\delta(\mathbf{A} - \mathbf{x})$ is two dimensional delta function on surface A. The deformation moment tensor is, from eq. (4),

$$D_{jk}(\mathbf{x}, t) = \{\lambda\ [u_m]\ \nu_m\ \delta_{jk} + \mu\ ([u_j]\ \nu_k + [u_k]\ \nu_j)\}\ \Delta A, \qquad (6)$$

where ΔA is the area of surface A. Using the trace of moment tensor, the volume ΔV of microcrack and the angle θ between $[u_i]$ and ν_i can be represented as

$$\Delta V = [u_m]\ \nu_m\ \Delta A = D_{ii}\ /\ (3\lambda + 2\mu), \qquad (7)$$

$$\cos\theta = [u_m]\ \nu_m\ /\ ([u_k]\ [u_k])^{1/2}. \qquad (8)$$

Acoustic Emission Signals

The detected signals of acoustic emission are generally different from the displacement field because of the response function of the measuring system, which is shown in Fig. 2. Denoting the response function in the i-direction at the position $\mathbf{x}$ on the surface by $S_i(\mathbf{x}, t)$, the detected signals $V(\mathbf{x}', t)$ due to moment tensor $D_{jk}(\mathbf{x}, t)$ can be expressed as (Kishi et al., 1983), form eq. (2),

$$V(\mathbf{x}', t) = S_i(\mathbf{x}', t) * G_{ij,k}(\mathbf{x}', \mathbf{x}, t) * D_{jk}(\mathbf{x}, t). \qquad (9)$$

EXPERIMENTAL SYSTEM

Figure 3 shows the block diagram of the multichannel AE detection and recording system. The transducer P50 (PAC) has a piezoelectric element of about 1 mm and a broad-band response up to 2 MHz. The output from each transducer is amplified 20 or 40 dB by the low noise type preamplifier 9913

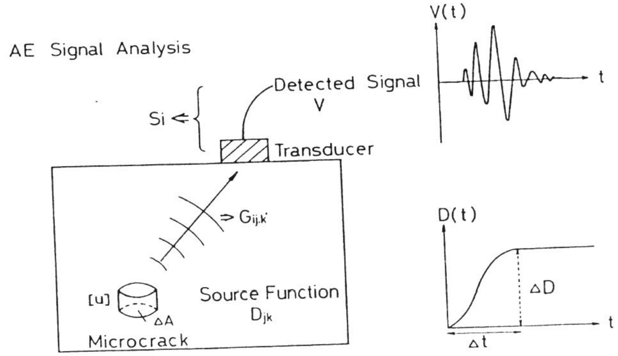

Fig. 2. The relation between source function D_{jk} and detected signal V in acoustic emission signal processing, where $G_{ij,k}$ is a dynamic Green's Function and S_i is a response function of measuring system.

(NF) with a frequency response, DC-20MHz, and then digitized and stored by the wave memory AE9620 (NF) with the maximum sampling rate of 20 MHz, resolution of 10 bits and the record length of 2048 points. Data from the wave memory are transferred via a GP-IB interface and stored on magnetic disc in the model 350 computer (HP). The transducers and measuring system are calibrated using a breaking pencil lead (Hsu et al., 1977). The AE analyzer AE9600 (NF) is also used to measure the conventional AE parameters of events and peak amplitude. The output from the transducer P50 (PAC) is fed into the AE analyzer AE9600 and the conventional AE parameters are stored on magnetic disc in a model 216 computer (HP) with the external parameters of load and COD. Each dynamic Green's function of the compact tension specimen concerning each source location which is calculated by a finite difference method, are transferred via a RS232C interface and stored on magnetic disc in the model 350 computer (HP).

ANALYSIS METHOD

Three Dimensional Source Location

The location of each source event is determined by measuring the differences in P-wave arrival time between two transducers. Suppose that Δt_{ij} is the difference in the P-wave arrival time between i-th and j-th transducers. Let $\mathbf{r}^i$ denote the transducer positions ($1 \leq i \leq P$) and $\mathbf{r}$ denote the location of the source, where P is the total number of channel. We can represent the equation for source location as

$$\alpha \, \Delta t_{iP} = |\mathbf{r} - \mathbf{r}^i| - |\mathbf{r} - \mathbf{r}^P|, \qquad 1 \leq i \leq P-1, \tag{10}$$

where α is the longitudinal velocity. If $P \geq 4$, then a nonlinear least-square method can be used to solve the eq. (10) for source location $\mathbf{r}$.

Calculation of Green's Function of Media

The Green's function which has the complex boundary conditions can be obtained only by the numerical simulation method. We simulate the dynamic Green's function of compact tension specimen by a finite difference method (Fukunaga et al., 1986). The finite difference formulations for equations of motion are derived by replacing the derivatives of the equation of motion with central differences for inner points. The one-sided approximations are

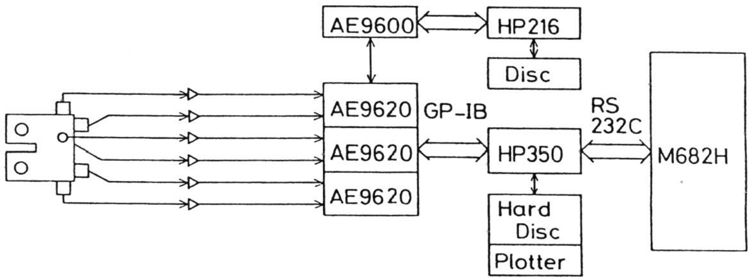

Fig. 3. The block diagram of the multichannel acoustic emission detection and recording system.

used for the free boundary conditions. In order to produce the moment $D_{jk}(\mathbf{x}, t)$ with force in the j-direction and arm in the k-direction at inner position $\mathbf{x}$, we apply a single couple with magnitude of $D_{jk}(\mathbf{x}, t)/\Delta l$ in the k-direction at both forward and backward points of $\mathbf{x}$ in the j-direction. We calculate the response functions at each transducer's position due to nine components of moment tensor at the obtained location of each source.

Response Function of Measuring System

The transducers and measuring system are calibrated using a breaking pencil lead. Before the fracture toughness testing, the waveform data due to the breaking pencil lead at the surface of specimen are recorded. The Green's function corresponding to the braking pencil lead is calculated by a finite difference method. Then the response function of measuring system was obtained from the result of the deconvolution with the known source function of the a pencil breaking lead and the above Green's function.

Deconvolution in frequency domain

Eq. (9), which is a convolution integral equation in time domain, can be written as

$$u^i(t) = \sum_{j=1}^{J} g^{ij}(t) * d^j(t), \qquad i=1, \ldots, I, \quad j=1, \ldots, J, \tag{11}$$

where $u^i(t)$ is the waveform data due to microcracking, $g^{ij}(t)$ is the transfer function which is convoluted by the transfer function of measuring system and Green's function of media, and $d^j(t)$ is the unknown moment tensor. Applying Laplace transform to this equation, we can find a discrete convolution integral equation in frequency domain as

$$\tilde{u}^i_n = \sum_{j=1}^{J} \tilde{g}^{ij}_n \, \tilde{d}^j_n, \qquad i=1, \ldots, I, \quad n=1, \ldots, N, \tag{12}$$

where $\tilde{}$ means Laplace transform. The algorithm to obtain moment tensor components is developed as follows:

(1) Both $u^i(t)$ and $g^{ij}(t)$ are respectively converted into $\tilde{u}^i_n$ and $\tilde{g}^{ij}_n$ by Laplace transform.

(2) Solving the linear eq. (12), $\tilde{d}^j_n$ is calculated.

(3) Using inverse Laplace transform, d^j_k is obtained from $\tilde{d}^j_n$.

In connection with the Laplace transform the time function has to be multiplied with $e^{-\delta t}$, so the discrete convolution error can be neglected if one chooses a suitable value for δ. As both transforms are performed by using the algorithm of the fast Fourier transform (FFT) (Krings et al., 1979), the calculation time of deconvolution can be shorter than that of the algorithm in time domain.

Evaluation of Microcrack

Assuming that a microcrack is a disc-like crack subject to a normally applied stress σ, we can state the crack volume as (Hutchinson, 1987)

$$\Delta V = 16\, a^3 \sigma \,(1 - \nu^2) / 3E, \tag{13}$$

where a is the crack radius, E is the Young's modulus, and ν is the Poisson's ratio. The crack radius a is, from eq. (7) and (13),

$$a = \{3\ (1 - 2\nu)\ D_{ii}\ /\ 16\ (1 - \nu^2)\ \sigma\}^{1/3}. \tag{14}$$

RESULTS AND DISCUSSION

Location

Figure 4(a) shows the location data of ASTM A470 steel in fracture toughness test with 1TCT specimen, which are plotted in projection of the xz and yz planes. The experimental error on each coordinate is estimated to be approximately 1 mm. It can be seen from Fig. 4(a) that source events are generated along the fatigue pre-crack approximately horizontally. All of sources are located within 1 mm of the crack tip. The dimension of plastic zone is about 0.5 mm, from the results of yield stress 616 MPa and fracture toughness 60 $MNm^{-3/2}$. Thus AE sources are believed to be microcracks in the plastic zone in consideration of error of source location, and so it will be possible to determine the dimension of plastic zone from the results of source location.

Figure 4(b) shows the location data of the sintered Si_3N_4 using a half size of a standard 1 inch thickness compact tension specimen with 25 mm thickness (0.5-1TCT) and the notch of 0.1 mm width. The experimental error on each coordinate is estimated to be approximately 1.2 mm from a sampling rate of 20 MHz and a longitudinal velocity in this material. It can be seen that source events are generated along the notch approximately horizontally, but it is more difficult in ceramics than in metals to estimate source location of microcracks because of the higher longitudinal velocity.

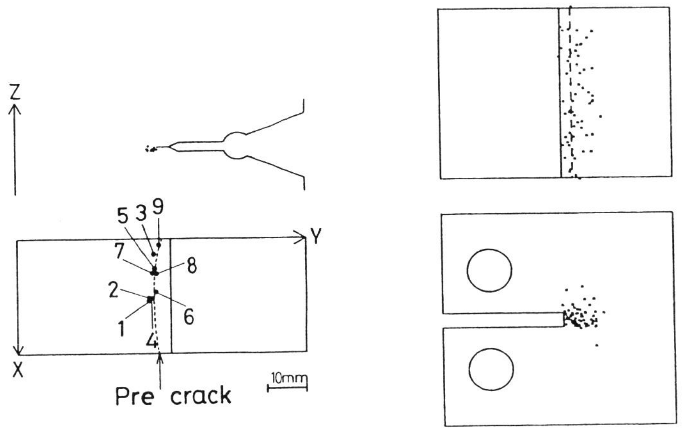

(a) (b)

Fig. 4. (a) The results of three dimensional location of acoustic emission sources detected during fracture toughness testing in ASTM A470 steel. (b) The results of three dimensional location of acoustic emission sources detected during fracture toughness testing in Si_3N_4.

Moment Tensor

Moment tensor D_{jk} are determined by the deconvolution method using some time points from P-wave arrival in the sintered Si_3N_4. Figure 5(a) shows an example of moment tensor D_{jk}. As shown in Fig. 5(a), a microcrack is generated with a rise time of about 0.2 μs. It is well known that solution by deconvolution method has less convergence, and deconvolution in the presence of noise expand error of solutions (Michaels et al., 1985). The whole errors in the moment tensor components could be likely to be estimated more than 10 %.

Microcrack

Applying the nonlinear least-square method to the eq. (6), the displacement discontinuity $[u_i]$ and the normal ν_i are obtained from the determined moment tensor D_{jk}. Figure 5(b) indicates that the inclination of the microcrack

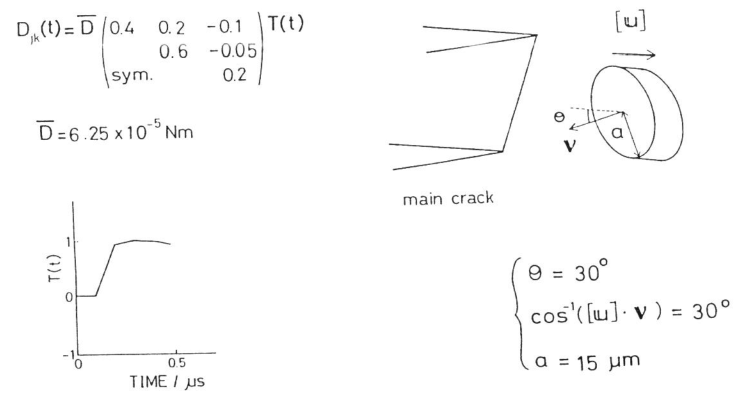

(a) (b)

Fig. 5. (a) The obtained result of moment tensor due to a microcracking in Si_3N_4.
(b) The results of the orientation, fracture mode and size of the microcrack.

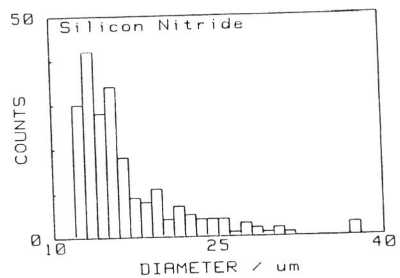

Fig. 6. The distribution of microcrack diameter evaluated by acoustic emission source characterization in Si_3N_4.

plane to the main crack surface is 90° and the inclination of the microcrack plane to the direction of the displacement discontinuity is 30°. This result has demonstrated that this analyzed microcrack is a crack with mixed fracture mode, which has more shear components than tensile. The crack radius a is calculated from the eq. (14) by assuming $\sigma = 3\sigma_{ys}$. Figure 6 shows that the value of radius a is estimated as 10 to 40 μm. The estimated value of radius a agrees well with the size of the secondary crack which is observed by scanning electron microscope at the location of source event. It can be concluded that the recorded AE events are the secondary cracks along the notch.

CONCLUSIONS

In this paper we developed the experimental analysis method by using AE signals in order to evaluate this microcracking quantitatively. Applied this method to fracture toughness testing of A470 steel and the sintered Si_3N_4, the following conclusions could be drawn.

(1) The experimental and analysis system due to AE source characterization, which can determine the moment tensor components in microcracking, was developed. This method is remarkable for the dynamic Green's function of finite media by finite difference computer simulation and for the deconvolution with multiple Green's function.

(2) Three dimensional location can clear that AE sources are located in the plastic zone near the pre-crack tip in A470 steel.

(3) From the obtained result of moment tensor, size, inclination of microcrack surface and fracture mode of microcrack were quantitatively evaluated.

(4) The observation by scanning electron microscope verified that these AE sources are identified as the secondary crack along the notch in the sintered Si_3N_4, which have a size of 10 - 40 μm.

REFERENCES

Aki, K. and P.G. Richards (1980). Quantitative Seismologiy Vol.1. W.H.Freeman and Company, San Francisco.

Enoki, M. and T. Kishi (1988). Theory and analysis of deformation moment tensor due to microcracking. Int. J. Fracture, to be published.

Fukunaga, Y. and T. Kishi (1986). Dynamic Green's function of finite media by finite difference method. In: Progress in acoustic emission III (K. Yamaguchi et al., Ed.), pp. 722-731. The Japanese society for non-destructive inspection, Tokyo.

Hsu, N.N., J.A. Simmons and S.C. Hardy (1977). An approach to acoustic emission signal analysis. Mater. Eval., 35, 100-106.

Hutchinson, J.W. (1987). Crack tip shielding by micro-cracking in brittle solids. Acta Metall., 35, 1605-1619.

Kishi, T. and T. Ohira (1983). Dynamic crack growth during pop-in fracture in 7975 aluminum alloy. Trans. Japan Inst. Metals, 24, 255-263.

Michaels, J.E. and Y.H. Pao (1985). The inverse source problem for an oblique force on an elastic plate. J. Acoust. Soc. Am., 77, 2005-2011.

Mura, T. (1982). Micromechanics of Defects in Solids. Martinus Nijhoff Publishers, The Hague.

Scruby, C.B., K.A. Stacey and G.R. Baldwin (1986). Defect characterisation in three dimensions by acoustic emission. J. Phys. D, 19, 1597-1612.

Wadley, H.N.G., C.B. Scruby and G. Shrimpton (1981). Quantitative acoustic emission source characterization during low temperature cleavage and intergranular fracture. Acta Metall., 29, 399-414.